TIME-LAPSE SEISMIC IMAGING BY LINEARIZED JOINT INVERSION

A DISSERTATION
SUBMITTED TO THE DEPARTMENT OF GEOPHYSICS
AND THE COMMITTEE ON GRADUATE STUDIES
OF STANFORD UNIVERSITY
IN PARTIAL FULFILLMENT OF THE REQUIREMENTS
FOR THE DEGREE OF
DOCTOR OF PHILOSOPHY

Gboyega Ayeni
November 2011

Contents

Chapter 1

Introduction

Time-lapse (4D) seismic imaging has become an established technology for monitoring changes in subsurface reservoir properties. In general, time-lapse seismic imaging involves repetition of similar seismic experiments over an evolving subsurface reservoir. Changes in the measured seismic reflection amplitudes and travel-times are then used to estimate changes in reservoir rock and fluid properties.

Over the past decade, the most important applications of time-lapse imaging have been in hydrocarbon reservoir monitoring. Widespread adoption of this technology as a reliable hydrocarbon reservoir monitoring tool can be attributed to improvements in seismic acquisition and imaging methods and to an improved understanding of the seismic responses of changing subsurface properties. Today, time-lapse seismic imaging is used to monitor changes in fluid flow, deformation, pressure, and saturation that are associated with hydrocarbon production and fluid injection. By providing information about changes within and around hydrocarbon reservoirs, time-lapse seismic imaging makes effective exploitation and management of hydrocarbon reserves possible. In addition, time-lapse seismic imaging has been widely applied to (and continues to be developed for) environmental applications, such as monitoring the flow of carbon dioxide sequestered in subsurface reservoirs.

Although time-lapse seismic imaging technology is now almost fully matured, several challenges still remain. In this dissertation, I explore some of these challenges and propose novel techniques to overcome them. Importantly, these techniques can attenuate artifacts in time-lapse images[1] that are caused by differences in acquisition parameters, obstructions, complex overburden and man-made noise. Therefore, even in the most difficult circumstances, we can obtain good-quality time-lapse images from which we can make reliable deductions about changes in subsurface reservoir properties.

TIME-LAPSE SEISMIC IMAGING CHALLENGES

Reservoir rock and fluid property changes can be obtained from seismic amplitude and/or travel-time changes. There is a wide range of published work on the most important considerations for time-lapse seismic imaging. For example, Batzle and Wang (1992) and Mavko et al. (2003) outline important rock and fluid relationships; Lumley (1995), Calvert (2005), and Johnston (2005) discuss important processing and practical applications; and Landro et al. (1999), Lefeuvre et al. (2003), Whitcombe et al. (2004), Zou et al. (2006), and Helgerud et al. (2011a) present several successful case studies. Because of the recorded successes in its applications, time-lapse seismic imaging has become an integral part of many hydrocarbon reservoir management projects.

In practice, differences in time-lapse seismic images caused by hydrocarbon production or fluid injection can be masked by non-repeatability artifacts (e.g., differences in acquisition geometry and ambient noise) or by uneven illumination due to complex overburden (e.g., a rugose salt canopy). Therefore, to correctly interpret time-lapse seismic images, such artifacts must be attenuated—a process commonly called seismic cross-equalization or cross-matching (Rickett and Lumley, 2001; Hall et al., 2005). Unless these artifacts are attenuated, it impossible to accurately relate seismic image differences to changes in reservoir properties.

[1] Note that throughout this dissertation, unless otherwise stated, a time-lapse image refers to the difference in reflectivity between a baseline image and a monitor image.

Although seismic cross-equalization methods are well developed and give reliable results in many practical applications, they fail where there are large inconsistencies between data sets or where the reservoir overburden is complex. In such scenarios, the inversion methods developed in this dissertation provide a way to attenuate artifacts that degrade time-lapse seismic images. Therefore, these methods improve our ability to estimate actual changes in reservoir properties from differences between seismic images. In addition, this dissertation discusses two common conventional time-lapse cross-equalization methods and shows how they can be improved. In the following sections, I outline some aspects of time-lapse seismic imaging that are considered in this dissertation.

Time-lapse *post-imaging* cross-equalization

Even where the acquisition parameters have been closely repeated for seismic baseline and monitor data sets, production-related image differences between them can still be masked by unwanted differences. These masking differences may be caused by factors such as changes in water velocity due to salinity or temperature changes, tidal differences, changes in source depth and/or source waveform, and uncorrelated ambient noise and multiples. In many cases, these differences may be strong enough to completely mask differences in time-lapse seismic images that are related to hydrocarbon production or fluid injection. As discussed above, in conventional time-lapse seismic processing, the process of attenuating these masking artifacts in time-lapse images is called seismic cross-equalization. In practice, depending on the data quality, seismic cross-equalization is applied at different stages during the processing sequence—before and/or after imaging.

Figure 1.1 shows the seismic baseline, monitor and time-lapse traces extracted from raw and cross-equalized data sets from a producing North Sea field. In this example, both the baseline and monitor data sets were acquired using state-of-the-art marine seismic acquisition technology, with the geometries repeated as closely as possible. However, small acquisition differences generate undesirable artifacts that mask production-related amplitude differences in the raw data (Figure 1.1(b)). In Figure 1.1(b), note that because of these undesirable artifacts, it is impossible to relate amplitudes in the time-lapse trace to production-related changes in the reservoir. Through seismic cross-equalization, these artifacts have been attenuated and production-related amplitude differences have been preserved (Figure 1.1(c)).

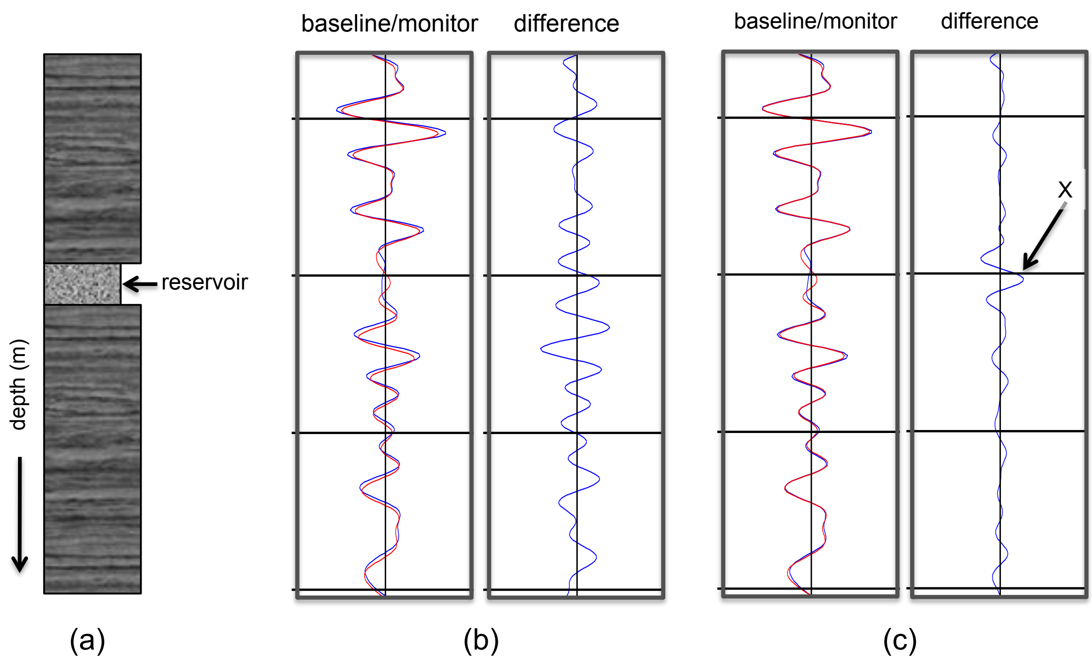

Figure 1.1: Comparison between migrated baseline and monitor seismic traces along a producing reservoir section (a). The superposed traces (left) and the difference (right) are shown before (b), and after (c) time-lapse cross-equalization. Note that before cross-equalization, small amplitude and phase differences contaminate the interesting time-lapse amplitude change between the traces (b). After careful cross-equalization, we obtain production-related amplitude change—indicated by the arrow X in (c)—which can then be transformed into reservoir property changes. chap1/. itr-4d

In this dissertation, I discuss how two widely used post-imaging cross-equalization methods—warping and match-filtering—can be improved. In addition, I show the processing steps applied to the raw data to obtain the result in Figure 1.1. Furthermore, I show practical scenarios where such processing steps become inadequate.

Geometry differences

In principle, if the acquisition and environmental conditions are perfectly repeated between surveys, the time-lapse seismic image can provide accurate information about production-induced changes in reservoir properties. For example, Figure 1.2 shows a typical marine acquisition geometry for a seismic baseline survey. In Figure 1.2, and throughout this dissertation, the target area is a region of interest around the reservoir, where production- or injection-induced changes are expected. Assuming a baseline data set was acquired prior to production, by acquiring the monitor data at a later date after production using the same geometry, the image difference between the baseline and monitor can provide a reliable measure of production-induced changes reservoir properties.

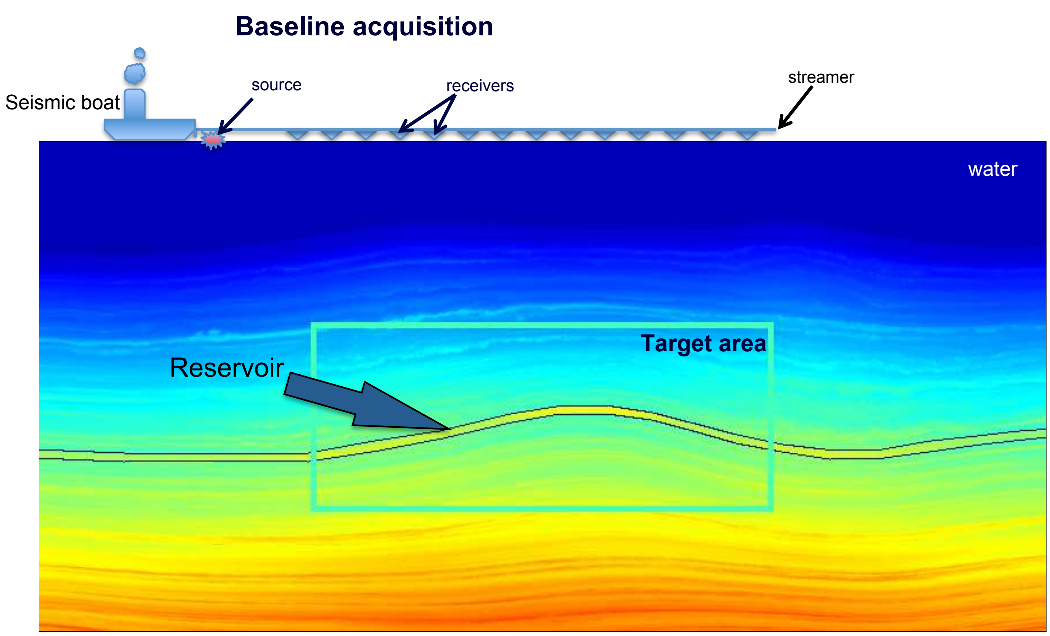

Figure 1.2: Cartoon illustrating a typical marine seismic acquisition geometry. The migrated baseline, monitor and time-lapse images for the boxed region (target area), obtained using the same geometry for both the baseline and monitor data sets, are shown in Figure 1.3. [**NR**] chap1/. acq-base

Figure 1.3 shows the migrated baseline and monitor images and the time-lapse image (monitor minus baseline) for the target area indicated in Figure 1.2. For this ideal case, amplitudes in the time-lapse image (Figure 1.3(c)) can be related directly to changes within the reservoir.

As noted earlier, where differences in the acquisition parameters are small, conventional time-lapse seismic processing methods (i.e., seismic cross-equalization methods) are sufficient to obtain reliable time-lapse images. However, these methods are usually unable to perfectly reconcile large differences in acquisition geometry between time-lapse data sets. Such large geometry differences can be caused by changes in acquisition systems, obstructions due to new production or drilling facilities, or natural environmental changes.

Figure 1.4 shows a practical time-lapse imaging problem in many oil and gas fields, where obstructions due to new production or drilling facilities prevent data recording in parts of the field. In many cases, these obstructions are absent during the baseline acquisition. As shown in Figure 1.5, the time-lapse image obtained in this scenario is different from the ideal case (Figure 1.3(c)). In this example, artifacts caused by acquisition geometry difference have masked the true reflectivity change, making it impossible to relate the reflectivity change to changes within the reservoir. Although new acquisition methods attempt to overcome this kind of problem, such methods are usually expensive (Stopin et al., 2011). In addition, whereas careful data regularization and processing methods can improve information derivable from data acquired with different geometries, these methods will fail where the geometry difference is large.

Artifacts exist in the time-lapse image (Figure 1.5) because the conventional imaging operator does not account fully for geometry differences between surveys. As described later in this chapter, linearized inversion provides a way to correct for geometry differences between seismic images. Furthermore, in chapter 4, I show that by applying the joint inversion methods developed in this dissertation to the data sets that produce the contaminated time-lapse image in Figure 1.5, we can obtain a time-lapse image similar in quality to that in Figure 1.3(c).

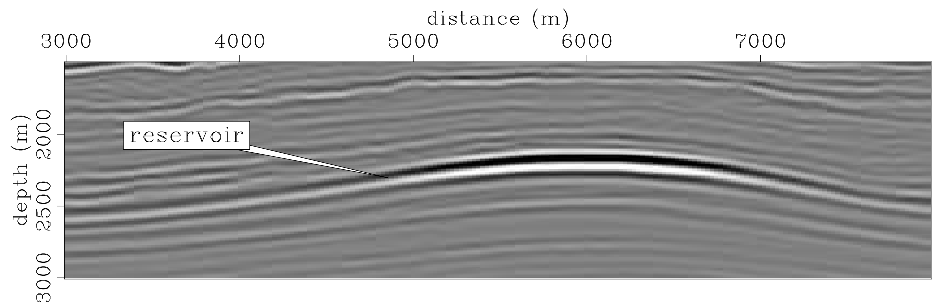

(a)

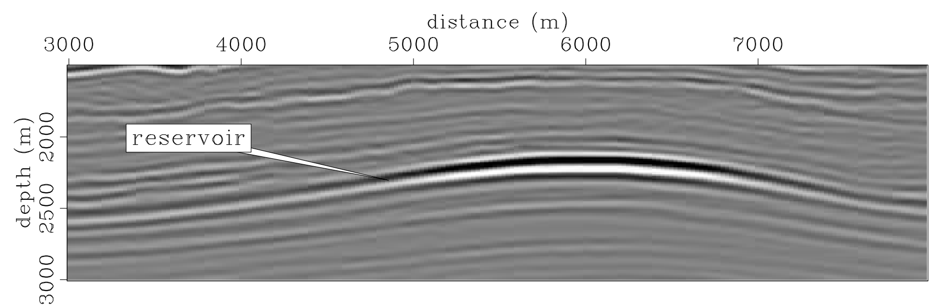

(b)

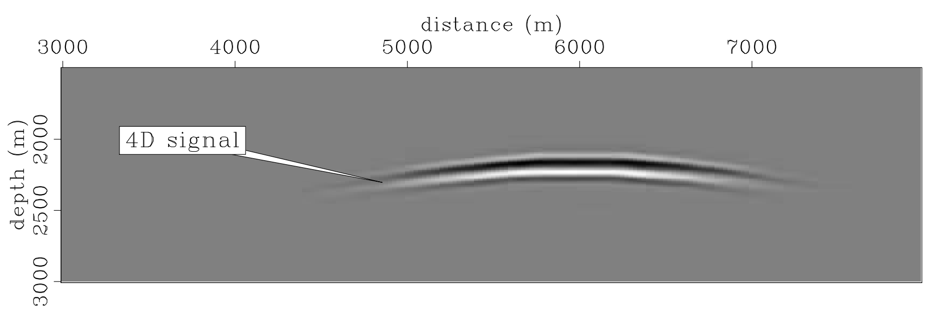

(c)

Figure 1.3: Migrated baseline image (a), monitor image (b), and time-lapse image (c) for the target area indicated in the numerical model in Figure 1.2. Note that in this ideal case, where acquisition geometries are repeated for both the baseline and monitor data sets, the amplitude difference in the time-lapse image is related only to changes within the reservoir. [**CR**] chap1/. s-mig-1l,s-mig-2l,s-mig–dl

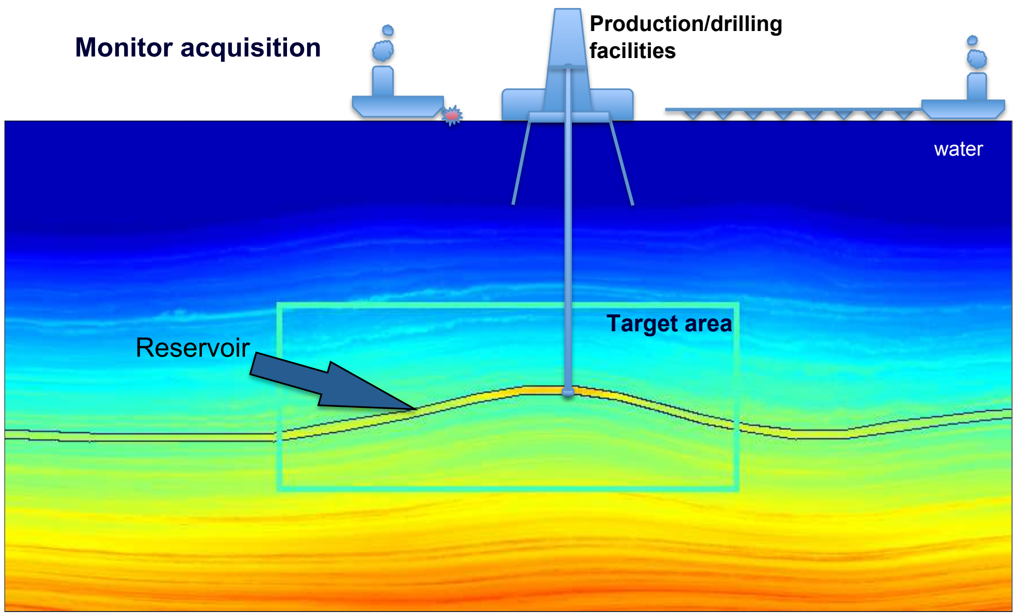

Figure 1.4: Cartoon illustrating how an obstruction in marine seismic acquisition affects data recording. Compare this cartoon to Figure 1.2. The time-lapse image for the target area, between the baseline image in Figure 1.3(a) and a monitor image with a gap caused by an obstruction, is shown in Figure 1.5. [**NR**] chap1/. acq-moni

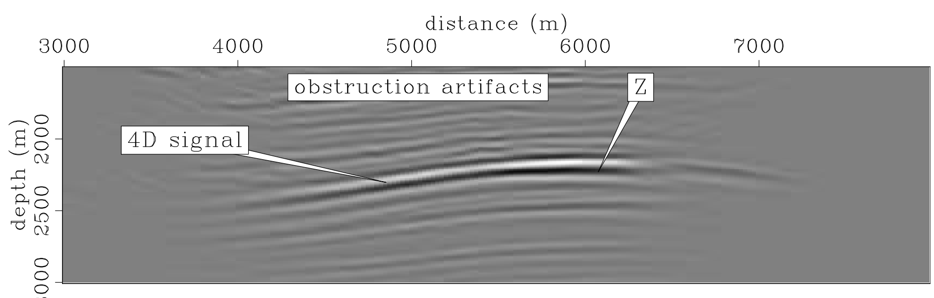

Figure 1.5: Time-lapse image obtained from a complete baseline data set (Figure 1.2) and an incomplete monitor data set (Figure 1.4). Note that, compared to the ideal time-lapse image in Figure 1.3(c), this image is highly contaminated with artifacts resulting from gap in the monitor acquisition geometry. To explain these artifacts, the impulse responses at point Z for the complete and incomplete geometries are studied later in this chapter. [**CR**] chap1/. s-mig-gap–dl

Overburden complexity

Conventional time-lapse processing methods are adequate in fairly simple geology—where, for example, simple migration methods (e.g., pre-stack time migration) image the targets with sufficient acccuracy. However, hydrocarbon exploration and production have shifted from relatively simple to complex geological environments (e.g., sub-salt reservoirs), where many of these methods are not adequate. Although recent advances in seismic acquisition have improved seismic imaging in these areas, reservoir monitoring remains difficult in complex geological environments.

Figure 1.6 shows an illustration of a reservoir located under a complex salt body. Because of the large contrast in seismic velocities between the salt body and surrounding sediments, unlike in the simple overburden example (Figure 1.2), only limited amount of seismic energy illuminates the sub-salt reservoir. Furthermore, such large contrast in seismic velocities, and the rugosity of the salt body cause highly uneven illumination of the reservoir.

Figure 1.7 shows the time-lapse image for the target area in Figure 1.6, obtained from baseline and monitor data sets that are modeled with the same acquisition geometry. Compared to the simple overburden example (Figure 1.3(c)), even with perfectly repeated acquisition geometries, the time-lapse image in this example is distorted. Because the conventional imaging operator does not account for these non-stationary distortions, it is difficult to accurately relate the observed reflectivity change to changes in reservoir properties. As described in the next section, linearized inversion provides a way to correct for these distortions in time-lapse seismic images caused by complex overburden.

In chapter 4, I show that by applying the joint inversion methods developed in this dissertation to the data sets that produce the distorted time-lapse image in Figure 1.7, we can obtain a time-lapse image similar in quality to that in Figure 1.3(c).

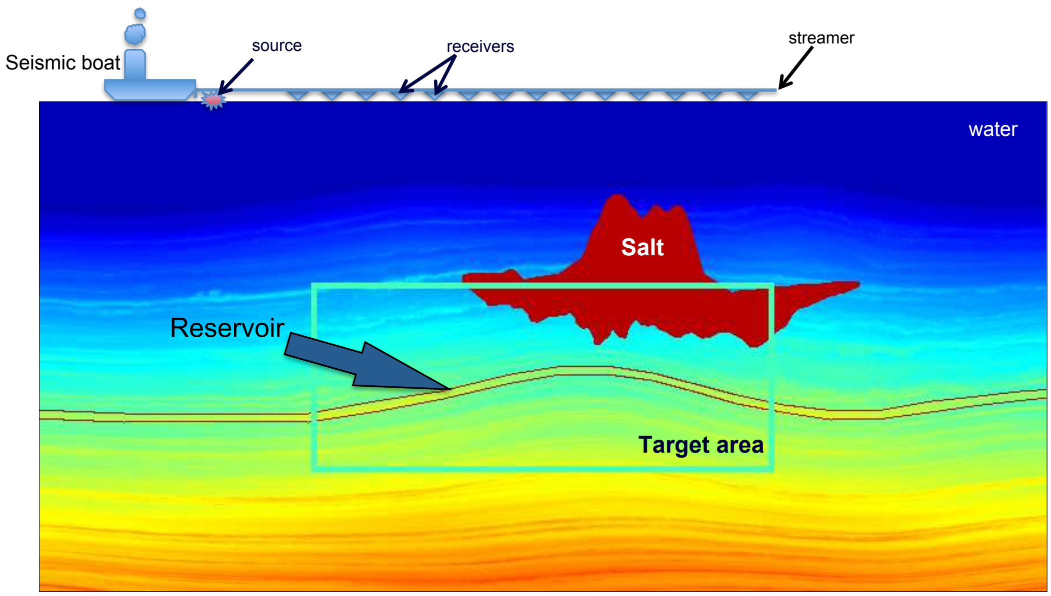

Figure 1.6: Cartoon illustrating a typical marine acquisition geometry over a complex earth model. Comparing this cartoon to Figure 1.2, note that in this subsurface model, the reservoir is located under a complex salt body. The time-lapse image for the target area, computed as the image difference between the baseline and monitor data sets, is shown in Figure 1.7. [**NR**]. chap1/. acq-moni-salt

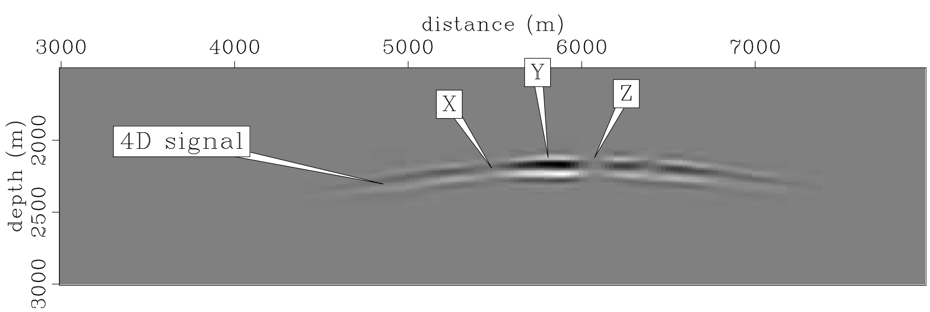

Figure 1.7: Time-lapse image between perfectly repeated baseline and monitor data sets from the numerical model in Figure 1.6. Note that, compared to the ideal time-lapse image in Figure 1.3(c), this image is highly distorted. These distortions in time-lapse amplitudes are caused by the uneven/irregular subsurface illumination associated with the complex overburden (Figure 1.9). To explain these distortions, the impulse responses at points X, Y, and Z are studied later in this chapter. [**CR**] chap1/. s-mig-salt–dl

Time-lapse imaging by inversion

As mentioned above, the conventional imaging operator does not account fully for differences in acquisition geometries and for band-limited wave-propagation effects. These limitations in the imaging operator cause artifacts and distortions in time-lapse images, such as those observed in Figures 1.5 and 1.7. Linearized inversion provides a way to correct for these artifacts and distortions. To understand these artifacts and how linearized inversion corrects them, let us consider briefly the impulse responses (point spread functions[2] (PSFs)) at image points identified in Figures 1.5 and 1.7.

Figure 1.8 shows the PSFs at point Z in Figure 1.5. As shown, at this image point,

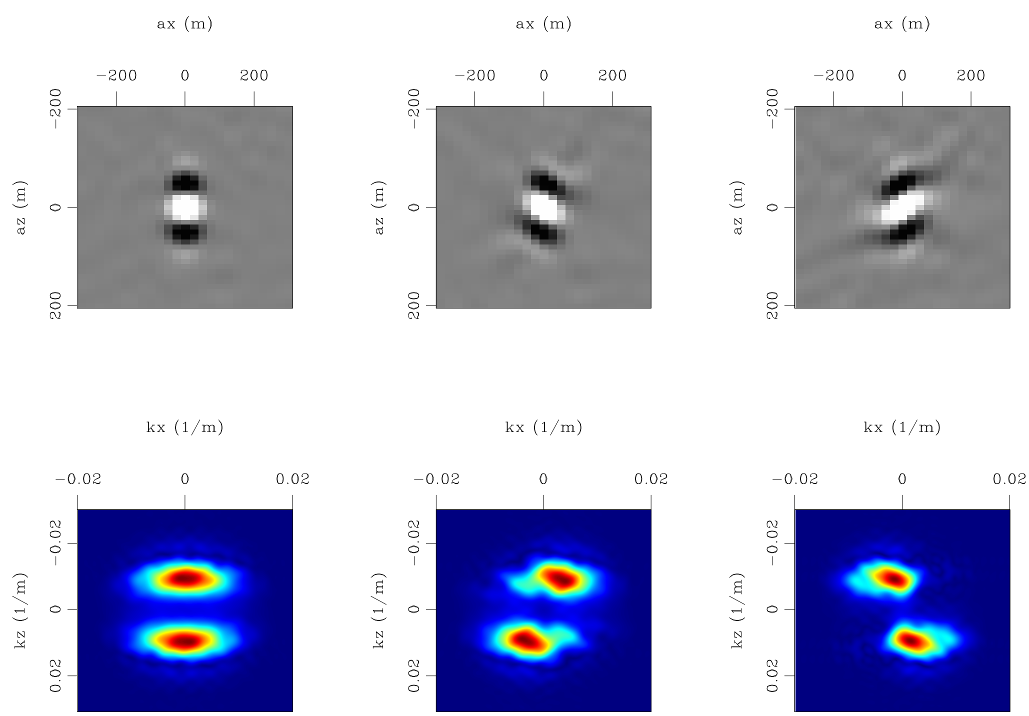

Figure 1.8: Point spread functions (PSFs) at point Z in Figure 1.5 in the spatial domain (top) and wavenumber domain (bottom). The left and middle panels are the PSFs for the baseline and monitor geometries respectively. The right panel shows the differences between the baseline and monitor PSFs resulting from differences in their geometries. [**CR**]. chap1/. sm-psf-a

[2]A point spread function describes the response of a subsurface spike to the imaging system.

because different acquisition geometries illuminate different ranges of wavenumbers, the spatial impulse response differ for the baseline and monitor. These differences in the impulse responses (or PSFs) caused by the geometry differences explain the artifacts observed in Figure 1.5. By removing the effects of these different PSFs, inversion attenuates geometry artifacts at each image point.

Figure 1.9 shows the PSFs at points X, Y, and Z in Figure 1.7. As shown, because of the complex overburden, even for these closely-spaced points, there are significant differences in spatial impulse responses (and hence in the range of illuminated wavenumbers). Large differences in the PSFs cause varying amounts of distortions in the time-lapse (Figure 1.7). Because inversion removes the effects of these non-stationary PSFs, it can attenuate distortions observed in time-lapse images.

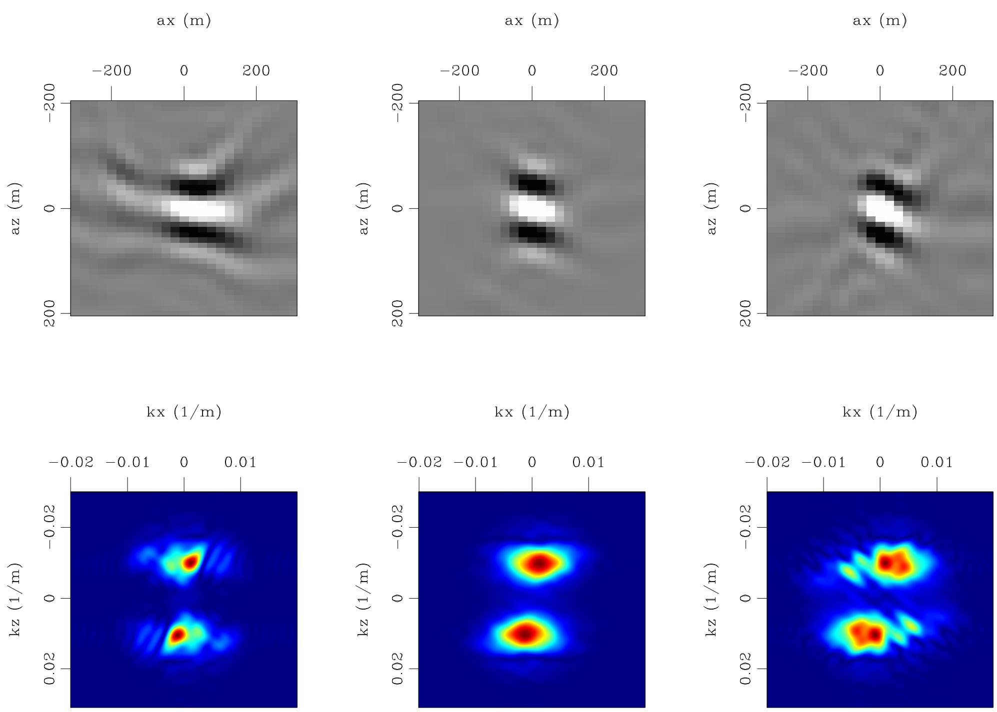

Figure 1.9: Point spread functions (PSFs) at points X, Y, and Z in Figure 1.7 in the spatial domain (top) and wavenumber domain (bottom). Although these points are located close to each other, because of the complex overburden, they differ significantly in the range of illuminated wavenumbers—hence the difference in the spreading. [**CR**]. chap1/. sm-psf-salt-a

As described above, linearized inversion can attenuate artifacts in time-lapse images caused by differences in acquisition geometries and by wave-propagation through complex overburden. However, because it is ill-posed, linearized inversion of seismic data is usually unstable. Therefore, in practice, unconstrained linearized inversion may lead to unsatisfactory results. However, for the time-lapse imaging problem, there are useful information about the subsurface geology, reservoir location and parts of the subsurface where changes are expected. In this dissertation, I show that including these a priori information as spatial[3] and temporal[4] constraints in the inversion provides stable and reliable time-lapse images.

DISSERTATION OVERVIEW AND CONTRIBUTIONS

The remaining chapters in this dissertation are organized according to the following outline:

Chapter 2 ***Time-lapse seismic cross-equalization*****:** Before introducing inversion methods in later chapters, it is important to understand conventional methods, their limitations, and how they can be improved. In this chapter, I focus on two post-imaging time-lapse seismic cross-equalization methods. First, I describe efficient multidimensional warping of time-lapse seismic images adapted from the method of Hale (2009). Then, using the method developed in Ayeni (2011), I show that selecting match-filtering parameters with an evolutionary algorithm leads to an improved match between time-lapse data sets. I apply the proposed methods to four time-lapse data sets from the Norne field.

Chapter 3 ***Joint least-squares wave-equation migration/inversion*****:** In this chapter, I discuss the theory of linear least-squares migration/inversion of seismic data (Nemeth et al., 1999; Clapp and Biondi, 2002; Kühl and Sacchi, 2003; Clapp, 2005; Valenciano, 2008; Tang, 2011), and how it can be extended to joint inversion of time-lapse data sets in both data and image domains. One

[3]Spatial constraints introduce a priori information about subsurface earth structure.
[4]Temporal constraints/coupling limit the difference between images from different surveys.

important advantage of solving a joint least-squares problem is that it allows the introduction of both spatial and temporal constraints. First, because seismic inversion is inherently ill-posed, these constraints help to stabilize the inversion. In addition, spatial and temporal constraints ensure that inverted the time-lapse images are geologically plausible. Therefore, compared to migration and separate inversion, joint least-squares inversion provides more reliable time-lapse images. I describe formulations of the regularized joint inversion in both the data and image domains. In general, the data-domain and image-domain inversion provide equivalent ways to solve the joint least-squares problem. However, one important advantage of image-domain inversion is that the problem can be solved for a small target around the reservoir.

Chapter 4 *Synthetic examples*: In this chapter, I apply the inversion methods developed in chapter 3 to various synthetic examples. In these examples, I demonstrate how joint least-squares inversion can be used to obtain high-quality time-lapse images in simultaneous-source data sets; how it can be used to correct for distortions in time-lapse images caused by complex overburden effects; and how it can be used to attenuate artifacts in time-lapse images caused by obstructions in acquisition geometries. I show that compared to conventional imaging by migration or separately regularized inversion, spatio-temporally regularized joint inversion provides more reliable time-lapse images.

Chapter 5 *2D field data examples*: In this chapter, I apply the joint image-domain inversion formulation developed in chapter 3 to subsets of a streamer time-lapse data set from the Norne field. As noted in the next section, and as demonstrated in chapter 5, the inversion method developed in this dissertation assumes that the data contain only primary reflections. Therefore, prior to inversion, the data must be carefully pre-processed. Preprocessing is necessary to ensure that as much as possible, the data satisfy the assumptions made in chapter 4. Using these data, I demonstrate how different pre-processing steps improve the time-lapse amplitude information and condition the data for inversion. In addition, I show that that linearized inversion can improve time-lapse images in conventional acquisition geometries. Furthermore, I demonstrate that this method can be used to attenuate obstruction artifacts in time-lapse images.

Chapter 6 ***3D field data examples*****:** In this chapter, I apply the joint image domain inversion formulation developed in chapter 3 to a full-azimuth Ocean-Bottom-Cable (OBC) data set from the Valhall Life of Field Seismic (LoFS) project. First, as in the 2D field data example in chapter 5, I demonstrate that linearized inversion can be used to attenuate obstruction artifacts time-lapse images between two and three surveys. In addition, I show that compared to migration, joint inversion provides results with improved resolution and more reliable information about production-related seismic amplitude changes. Finally, I demonstrate that because joint image domain inversion is cheap, we can use different regularization parameters to obtain several plausible time-lapse images of reservoir changes. This means that it is possible to introduce realistic constraints or prior knowledge in the computation of the time-lapse difference.

Chapter 7 ***Conclusions*****:** In this chapter, I summarize the most important results in this dissertation and I discuss some probable directions for future research.

ASSUMPTIONS AND LIMITATIONS

The joint least-squares formulations developed in this dissertation are subject to several assumptions and limitations. Below, I summarize the most important of these.

- Velocity and compaction: I assume that the background baseline velocity is accurate. Also, I assume that between surveys, velocity change relative to the background, and compaction relative to the reservoir size and depth are small. Where the velocity change and compaction are unavailable (or are not of interest), I assume that errors introduced by imaging all data sets with the baseline velocity can be removed by post-imaging warping/alignment.

- Noise: In deriving the inversion formulations in this dissertation, I assume a linear *primaries-only* approximation to the wave-equation. Therefore, prior to inversion, all data sets must be pre-processed to remove correlated and uncorrelated noise. I assume that residual noise in the data sets is of smaller magnitude than the time-lapse signal of interest.

- Reservoir property changes: Throughout this dissertation, inversion is limited to the estimation of changes in reflectivity amplitudes. Changes in actual rock properties (e.g., saturation and permeability) can be obtained from the inverted time-lapse amplitudes. One possible direction of future research is an extension of the formulations developed in this dissertation to direct inversion of reservoir property changes.